Molecular Therapy
Methods & Clinical Development
Original Article

AAV2/6 Gene Therapy in a Murine Model of Fabry Disease Results in Supraphysiological Enzyme Activity and Effective Substrate Reduction

Makiko Yasuda,[1,3] Marshall W. Huston,[2,3] Silvere Pagant,[1] Lin Gan,[1] Susan St. Martin,[2] Scott Sproul,[2] Daniel Richards,[2] Stephen Ballaron,[2] Khaled Hettini,[2] Annemarie Ledeboer,[2] Lillian Falese,[2] Liching Cao,[2] Yanmei Lu,[2] Michael C. Holmes,[2] Kathleen Meyer,[2] Robert J. Desnick,[1] and Thomas Wechsler[2]

[1]Department of Genetics and Genomic Sciences, Icahn School of Medicine at Mount Sinai, New York, NY, USA; [2]Sangamo Therapeutics, Inc., Brisbane, CA 94005, USA

Fabry disease is an X-linked lysosomal storage disorder caused by mutations in the alpha-galactosidase A (*GLA*) gene, which encodes the exogalactosyl hydrolase, alpha-galactosidase A (α-Gal A). Deficient α-Gal A activity results in the progressive, systemic accumulation of its substrates, globotriaosylceramide (Gb3) and globotriaosylsphingosine (Lyso-Gb3), leading to renal, cardiac, and/or cerebrovascular disease and early demise. The current standard treatment for Fabry disease is enzyme replacement therapy, which necessitates lifelong biweekly infusions of recombinant enzyme. A more long-lasting treatment would benefit Fabry patients. Here, a gene therapy approach using an episomal adeno-associated viral 2/6 (AAV2/6) vector that encodes the human *GLA* cDNA driven by a liver-specific expression cassette was evaluated in a Fabry mouse model that lacks α-Gal A activity and progressively accumulates Gb3 and Lyso-Gb3 in plasma and tissues. A detailed 3-month pharmacology and toxicology study showed that administration of a clinical-scale-manufactured AAV2/6 vector resulted in markedly increased plasma and tissue α-Gal A activities, and essentially normalized Gb3 and Lyso-Gb3 at key sites of pathology. Further optimization of vector design identified the clinical lead vector, ST-920, which produced several-fold higher plasma and tissue α-Gal A activity levels with a good safety profile. Together, these studies provide the basis for the clinical development of ST-920.

INTRODUCTION

Fabry disease (OMIM: 301500), an X-linked lysosomal storage disorder, results from the deficient activity of the exogalactosyl hydrolase, alpha-galactosidase A (α-Gal A; GenBank: NP_000160.1).[1] Deficiency in α-Gal A activity results in progressive, systemic accumulation of its primary substrate, globotriaosylceramide (Gb3), and its deacylated derivative, globotriaosylsphingosine (Lyso-Gb3), particularly in the lysosomes of vascular endothelial cells, renal (i.e., epithelial, endothelial, and mesangial) cells, and cardiomyocytes.[2–5] There are two major clinical subtypes. Type 1 classic affected males have essentially no residual α-Gal A activity and typically present in childhood or adolescence with acroparesthesias, angiokeratomas, hypohidrosis, non-specific gastrointestinal symptoms, and a characteristic corneal dystrophy. The natural course of the disease is characterized by progressive deposition of the substrates, leading to cardiac, renal, and/or cerebrovascular disease and early demise in the fourth or fifth decade of life.[1,6,7] Affected males with mutations encoding low levels of residual α-Gal A activity have type 2 later-onset phenotype; these subjects lack the characteristic early manifestations in type 1 males and typically develop kidney, cardiac, and/or cerebrovascular disease in the fourth to sixth decades.[8–10] Heterozygous females can be as symptomatic as their affected male relatives or asymptomatic, due primarily to random X chromosome inactivation.[11]

Therapeutic options for Fabry disease are currently limited. For both type 1 and 2 patients, the standard of care is enzyme replacement therapy (ERT), which involves regular intravenous (i.v.) infusions of human recombinant α-Gal A enzyme.[12–14] Once in the circulation, the recombinant enzyme is taken up by secondary tissues via mannose-6-phosphate (M6P) receptor-mediated endocytosis. Although ERT is effective, especially if initiated early in the disease,[13,15–17] the relatively short half-life of recombinant enzyme necessitates a lifelong burden of infusions every 2 weeks.[13] In addition, a significant percentage of type 1 males on ERT eventually generate antibodies to recombinant enzyme, which, if neutralizing, can reduce the efficacy of treatment.[18,19] Recently, an oral pharmacological chaperone therapy (Migalastat) was approved for the treatment of Fabry disease in a number of counties.[20] However, a major limitation of this approach is that only a portion of the alpha-galactosidase A gene (*GLA*) mutations are amenable, most causing the type 2 phenotype.[21–23] Thus, a more long-lasting treatment for Fabry disease that is effective and safe is desirable.

Recombinant adeno-associated viral (rAAV) vectors have shown great promise in both preclinical and clinical trials to efficiently deliver therapeutic transgenes to the liver, with sustained transgene expression for

Received 9 March 2020; accepted 2 July 2020;
https://doi.org/10.1016/j.omtm.2020.07.002.

[3]These authors contributed equally to this work.

Correspondence: Marshall W. Huston, PhD, Sangamo Therapeutics, Inc., 7000 Marina Blvd., Brisbane, CA 94005, USA.
E-mail: mhuston@sangamo.com

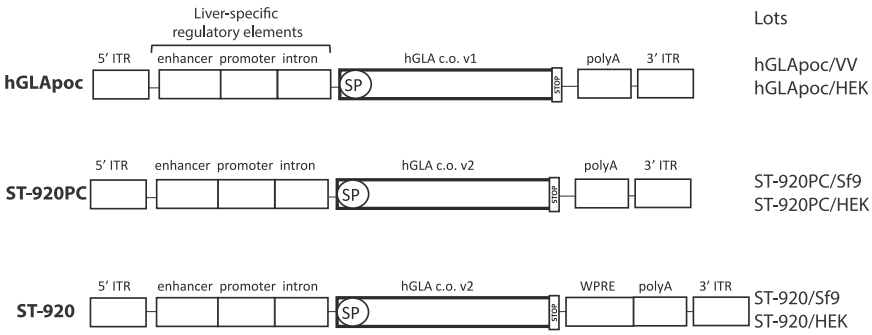

Figure 1. Schematic Showing the Various AAV2/6 hGLA Vectors Used in These Studies

Three different *GLA* expression cassettes were packaged into AAV2/6 vectors and assessed *in vitro* and *in vivo*. All cassettes contain liver-specific enhancers and promoters, as well as a chimeric intron, codon-optimized human *GLA* cDNA and polyA sequence, flanked by AAV2 inverted terminal repeats (ITRs). The first expression cassette evaluated was hGLApoc. ST-920PC has an identical expression cassette to hGLApoc but has an alternate *GLA* cDNA codon optimization sequence, which leads to higher transgene expression in hepatocytes. ST-920, the final lead vector, has the same improved *GLA* cDNA codon optimization scheme as ST-920PC and features a 3′ enhancer element, the WPRE, to further increase transgene expression. The three expression cassettes were packaged into AAV2/6 vectors manufactured using either a HEK293 or Sf9/rBV production system: the lots of each cassette tested are listed on the far right side of the figure. hGLA c.o. v1, human *GLA* codon optimization scheme version #1; hGLA c.o. v2, human *GLA* codon optimization scheme version #2; SP, signal peptide.

up to 7 years in hemophilia B patients.[24] Here we describe a series of preclinical studies using liver-targeted rAAV2/6 vectors encoding the human *GLA* cDNA (AAV2/6-hGLA) driven by liver-specific promoters and enhancers. The efficacy and safety of AAV2/6-mediated gene therapy were evaluated using a well-established mouse model of Fabry disease (*Gla* KO) that lacks endogenous α-Gal A expression and progressively accumulates Gb3 and Lyso-Gb3 systemically.[25] Initial proof of concept was established in a 6-month dose titration study in Fabry mice. A hybrid 3-month pharmacology and toxicology study showed that ST-920PC, a clinical-scale-manufactured AAV2/6-hGLA vector, resulted in markedly increased plasma and tissue α-Gal A activities and essentially normalized substrate concentrations in key tissues with no apparent adverse effects. *In vitro* and *in vivo* studies to optimize vector design showed that addition of a 3′-enhancer element, a mutated variant of the Woodchuck hepatitis virus (WHP) post-transcriptional regulatory element (WPRE), further increased transgene expression of the therapeutic vector. This improved construct was selected as the clinical lead vector, designated ST-920.

RESULTS

6-Month Pharmacology Study with an AAV2/6-hGLA Vector Achieves Effective Substrate Clearance in Key Tissues of Adult Fabry Mice and Establishes Proof of Concept for This Approach

To evaluate the potential of gene therapy for Fabry disease, we generated a proof-of-concept AAV2/6 vector containing a codon-optimized human *GLA* cDNA and liver-specific promoter and enhancer elements by a small-scale Sf9 insect cell/recombinant baculovirus (Sf9/rBV) production method (designated hGLApoc/VV vector; Figure 1), and its pharmacodynamic activity was assessed in a 6-month dose-finding study in immunosuppressed Fabry male mice. Initial efforts determined that a single i.v. administration of the hGLApoc/VV vector effectively transduced the livers of the Fabry mice. Dose-dependent increases in vector DNA copy numbers were observed in liver 180 days following administration of hGLApoc/VV at a dose of 1.25E+11, 2.5E+11, 5E+11, 1E+12, 2E+12, or 5E+12 vector genomes (vg)/kg ($n \geq 4$; Figure S1A). In line with these findings, transgene-specific hGLA mRNA expression also increased in a dose-dependent manner in the livers of treated Fabry mice (Figure S1B). Western blot analyses using an anti-human α-Gal A antibody detected a band approximately 50 kDa, consistent with the mature human α-Gal A protein,[26] in liver from Fabry mice treated with vector doses of 2E+12 vg/kg or higher, but not in wild-type or the untreated Fabry mouse controls (Figure 2A). Thus, i.v. administration of hGLApoc/VV vector effectively transduced Fabry mouse livers, resulting in hepatic expression of the mature human α-Gal A protein.

Fabry mice administered hGLApoc/VV at 1.25E+11, 2.5E+11, 5E+11, 1E+12, 2E+12, or 5E+12 vg/kg were assessed every 1–2 weeks for plasma α-Gal A activity. These animals showed sustained, dose-dependent increases for the duration of the study (Figure 2B), indicating that the liver-expressed enzyme was active and continuously secreted into the bloodstream. At 180 days post-treatment, mean plasma activity was 12.3 ± 1.2 nmol/h/mL (mean ± SEM) in the lowest dose group (1.25E+11 vg/kg), comparable with mean wild-type levels of 9.9 ± 1.3 nmol/h/mL. In contrast, mean plasma activity in the highest dose group (5E+12 vg/kg) was 257.5 ± 72.6 nmol/h/mL, corresponding to 26-fold over mean wild-type levels. Of note, the 2E+12 vg/kg dose group was administered a last cyclophosphamide injection on day 140 post-treatment and then taken off immune suppression to evaluate whether the Fabry mice develop antibodies against the transgene-expressed human α-Gal A enzyme or whether the mice can instead be tolerized to the human α-Gal A enzyme, as has been reported in previous preclinical AAV gene therapy studies.[27,28] Despite discontinued immunosuppression, plasma α-Gal A activities remained stably elevated in these mice, with mean plasma activities of 262, 248, 215, and 232 nmol/h/mL at days 126, 140, 152, and 168, respectively (Figure 2B).

To determine whether α-Gal A enzyme secreted from liver into the bloodstream was being taken up by distal secondary tissues and was able to effectively clear the accumulated substrates, we quantified Gb3 and Lyso-Gb3 concentrations in the heart and kidney, the two key sites of pathology in Fabry disease,[1] at 180 days post-treatment. In general, tissue and plasma substrate concentrations correlated inversely with vector dose (Figure 2C). In heart, Lyso-Gb3 concentrations were essentially normalized, and Gb3 levels were ≤20% of formulation buffer-treated Fabry controls in mice administered 1E+12 vg/kg or higher vector doses.

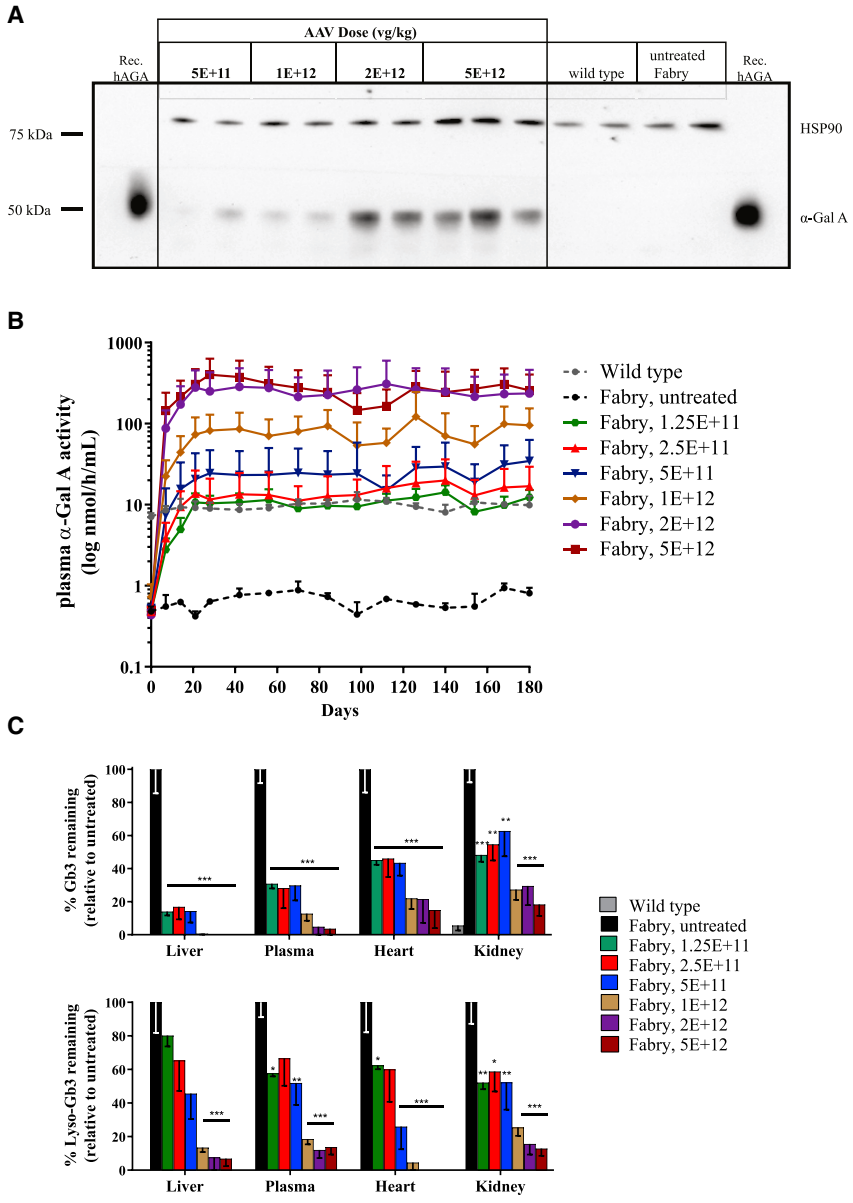

Figure 2. hGLApoc/VV Produces Continuous Supraphysiological Levels of α-Gal A in Plasma and Markedly Reduces Substrates in Key Tissues in Fabry Mice

Fabry male mice were i.v. administered hGLApoc/VV at doses ranging from 1.25E+11 to 5E+12 vg/kg and were euthanized for tissue collection at 180 days post-injection. Age- and sex-matched untreated wild-type and Fabry males were included as controls. (A) Representative western blot image showing expression of the mature 50-kDa α-Gal A enzyme in livers of hGLApoc/VV-treated Fabry mice. To avoid potential background signal from endogenous mouse α-Gal A in wild-type controls, we used an antibody raised specifically against the human enzyme. Recombinant human α-Gal A (Rec.hAGA) produced in CHO cells is shown to confirm the correct size and glycosylation pattern. A murine anti-heat shock protein 90 (HSP90) antibody was used as a loading control. (B) Plasma α-Gal A activities out to 180 days post-vector administration. (C) Remaining percentage (%) of plasma and tissue glycolipid substrates, Gb3 (top) and Lyso-Gb3 (bottom), relative to untreated Fabry mice. Data shown in (B) and (C) represent means ± SDs (n = 4–7). *p < 0.05, **p < 0.01, ***p < 0.001 versus untreated Fabry group, two-way repeated-measures ANOVA followed by Dunnett's multiple comparison test.

Significant substrate clearance was also achieved in kidney, particularly in the highest vector dose group, which had <20% of Gb3 and Lyso-Gb3 remaining relative to controls. The second and third highest dose groups (1E+12 and 2E+12 vg/kg) had <30% of Gb3 and Lyso-Gb3 remaining in their kidney compared with controls (Figure 2C). Plasma and liver Gb3 and Lyso-Gb3 were effectively decreased to levels that were <20% of controls in mice treated with 1E+12 vg/kg or higher doses.

Together, these data indicate that AAV2/6-mediated expression of α-Gal A was sustained long term in the plasma and tissues and effectively cleared the toxic substrates, Gb3 and Lyso-Gb3, from the key sites of pathology in the Fabry mice. The observation that mice in which immunosuppression was discontinued (2E+12 vg/kg group) maintained markedly elevated plasma α-Gal A levels suggests that these animals did not generate substantial levels of neutralizing antibodies against the human enzyme. Based on these findings, all studies described below were performed in the absence of an immunosuppression regimen.

AAV2/6-hGLA-Expressed Human α-Gal A Enzyme Is Highly Glycosylated and Delivered to Other Cells via M6P Receptors

An AAV2/6-hGLA vector designated ST-920PC/human embryonic kidney (HEK) was generated in HEK cells, and its efficacy was compared with that of hGLApoc/HEK in hepatoma cell lines and then in the Fabry mice. The ST-920PC expression cassette was similar in design to the hGLApoc cassette, except that the h*GLA* transgene had a different codon optimization sequence (Figure 1). The ST-920PC/HEK vector produced ~2- and ~7-fold higher supernatant α-Gal A activities upon transduction of human HepG2 cells and murine Hepa1–6 cells, respectively, relative to hGLApoc/HEK (Figure 3A). i.v. administration of 2E+12 vg/kg of each vector into Fabry mice showed that ST-920PC/HEK resulted in α-Gal A activities that were 4- to 11-fold higher than hGLApoc/HEK in the plasma and all tissues assessed, including liver, spleen, heart, and kidney (Figure 3B). Thus, ST-920PC achieved higher transgene activities, both *in vitro* and *in vivo*, and was selected for the subsequent pharmacology and toxicology studies.

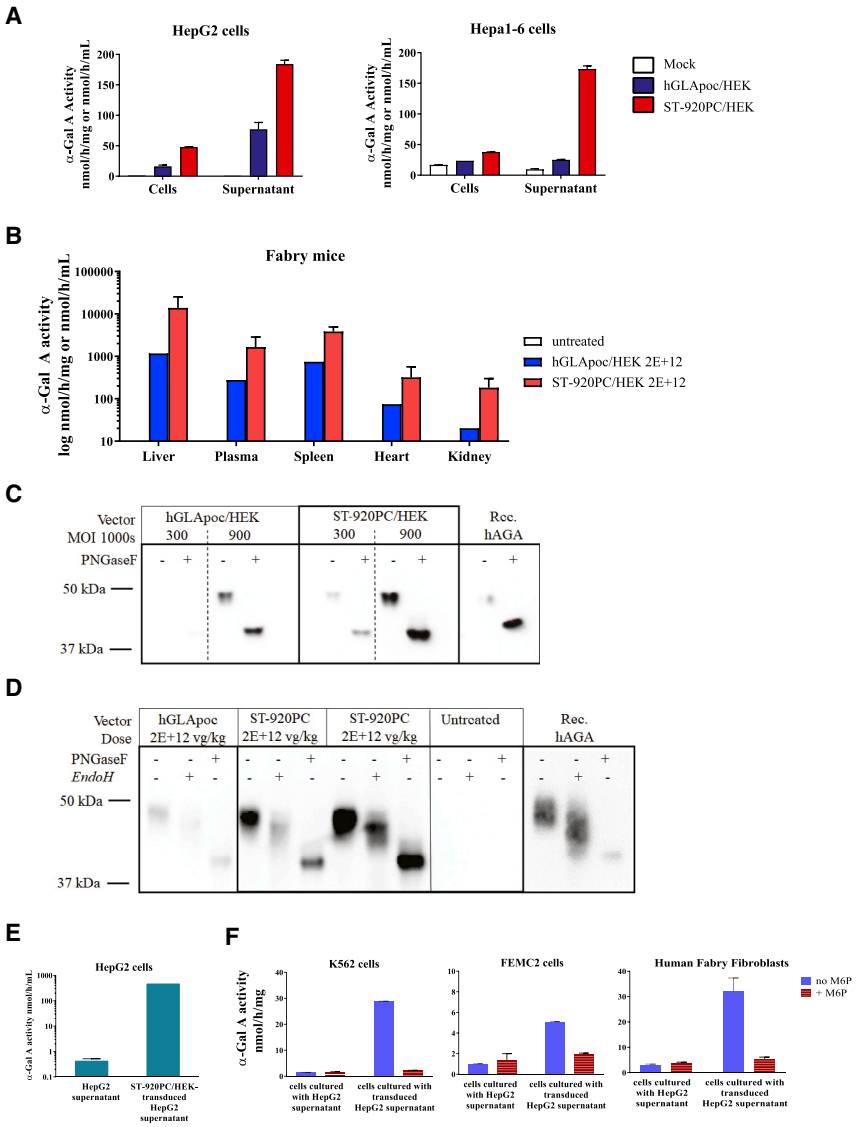

Figure 3. ST-920PC/HEK Is More Potent Than hGLApoc/HEK and Leads to Higher Expression of α-Gal A, which Is Taken Up by Cells via M6P Receptors

(A) Intracellular and supernatant α-Gal A activities in HepG2 (left) and Hepa1–6 cells (right), 6 days after transduction with hGLApoc/HEK or ST-920PC/HEK at an MOI of 300,000 vg/cell. Data represent mean ± SD of two biological replicates. (B) Plasma and tissue α-Gal A activities 2 months after Fabry males were dosed with 2E+12 vg/kg hGLApoc/HEK (n = 1) or ST-920PC/HEK (n = 4), or a formulation containing no AAV2/6 vector (untreated control, n = 4). (C) Representative western blot image showing α-Gal A protein, with and without PNGase F digestion, detected in the supernatants of HepG2 cells transduced with hGLApoc/HEK or ST-920PC/HEK vectors at an MOI of 300,000 or 900,000 vg/cell. Rec.hAGA produced in CHO cells is shown as a positive control. (D) Representative western blot image showing liver-produced α-Gal A protein with and without glycosidase digestion. Liver extracts of GLApoc/HEK- or ST-920PC/HEK-treated Fabry mice were digested with PNGase F or EndoH and probed for α-Gal A to compare the glycosylation patterns of AAV2/6-expressed α-Gal A with that of Rec.hAGA produced in CHO cells. To avoid potential background signal from endogenous mouse α-Gal A in wild-type controls, an antibody raised specifically against the human enzyme was used in both (C) and (D). (E) α-Gal A activity was markedly increased in the supernatants 5 days after HepG2 cells were transduced with ST-920PC/HEK at an MOI of 600,000 vg/cell. Mock-transduced HepG2 cell supernatant (HepG2 supernatant) served as a negative control. (F) Intracellular α-Gal A activities in (left to right) human leukemia K562 cells, Fabry mouse-derived immortalized aortic endothelial cells (FMEC2), and Fabry patient fibroblasts, determined 24 h following incubation with the α-Gal A-enriched supernatant, or mock-transduced HepG2 supernatant (negative control), in the presence or absence of 5 mM mannose-6-phosphate (M6P). Data represent mean ± SD of three biological replicates.

To assess the glycosylation status of the human α-Gal A enzyme expressed by the AAV2/6-hGLA vectors, supernatants of hGLApoc/HEK- or ST920PC/HEK-transduced HepG2 cells were digested with peptide-*N*-glycosidase F (PNGase F; Figure 3C). Similarly, livers isolated from hGLApoc/HEK- or ST920PC/HEK-treated Fabry mice were digested with PNGase F or endoglycosidase H (EndoH) and assessed by western blotting (Figure 3D). In both the cell supernatant and the liver, the AAV2/6-hGLA-expressed α-Gal A enzyme displayed deglycosylation patterns similar to those of recombinant human α-Gal A enzyme produced in Chinese hamster ovary (CHO) cells (Figures 3C and 3D). These findings indicated that the AAV2/6-hGLA-expressed α-Gal A enzyme is appropriately glycosylated, further supporting that the protein being expressed is the mature form.

Subsequently, we assessed whether cellular uptake of the AAV2/6-hGLA-expressed α-Gal A enzyme was mediated via M6P receptors. HepG2 cells were transduced with ST-920PC, and α-Gal A-enriched supernatant was collected 5 days post-transduction (Figure 3E). When human leukemia K562 cells, Fabry mouse-derived immortalized aortic endothelial cells (FMEC2), and Fabry patient fibroblasts were incubated with the α-Gal A-enriched supernatant in the absence of exogenous M6P, intracellular α-Gal A activities markedly increased, indicating that the enzyme was efficiently taken up by the cells (Figure 3F). Addition of 5 mM M6P sharply decreased uptake of the enzyme in all three cell lines, demonstrating that the AAV2/6-hGLA-expressed α-Gal A enzyme is taken up by cells via M6P receptors (Figure 3F).

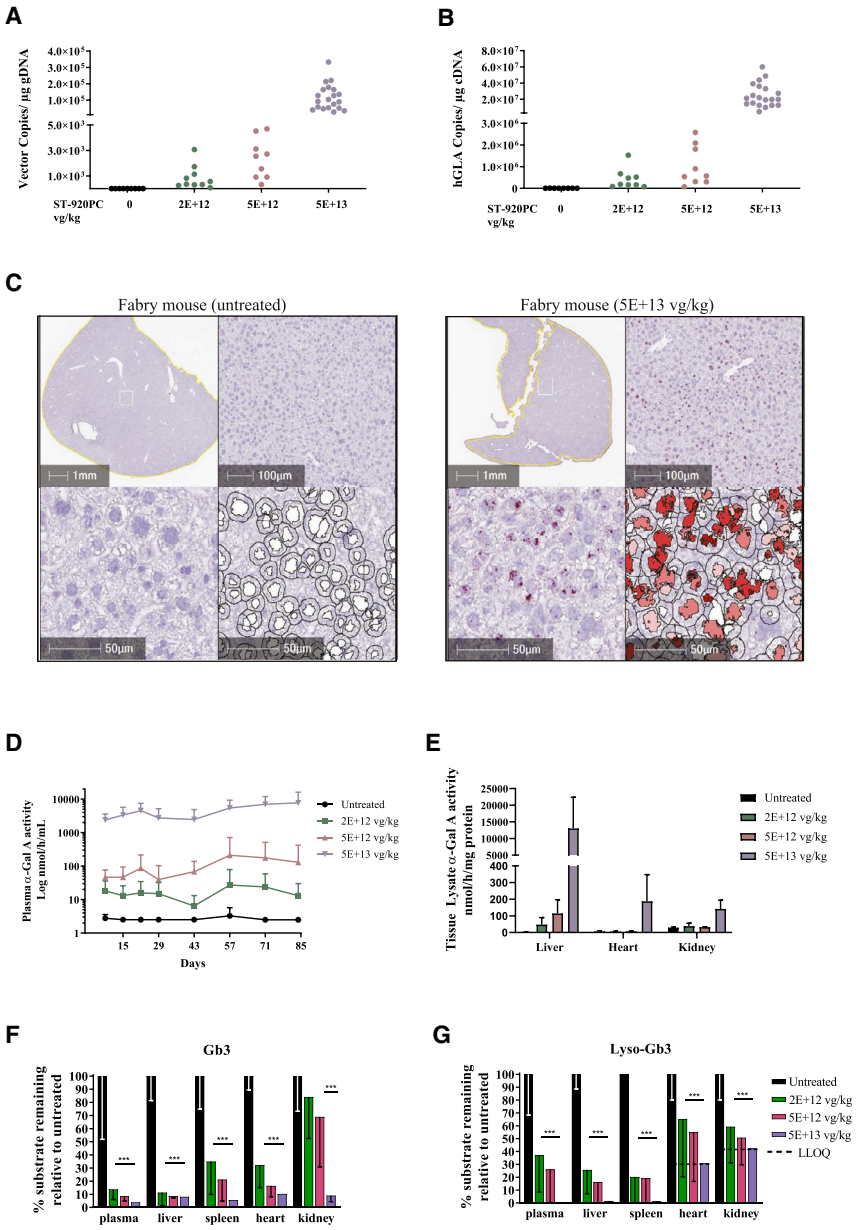

Figure 4. Clinical-Scale Manufactured ST-920PC/Sf9 Vector Results in Supraphysiological Levels of α-Gal A in Plasma and Tissues and Essentially Normalizes Substrates in Key Tissues in Fabry Mice

Fabry males were i.v. administered formulation buffer or the ST-920PC/Sf9 vector at doses of 2.0E+12 (low), 5.0E+12 (mid), or 5.0E+13 vg/kg (high), and tissues were collected at 90 days post-injection. (A and B) AAV vector genome (vg) copy numbers (A) and *GLA* mRNA copy numbers (B) were determined in the livers. (C) Representative images of liver sections hybridized with a DNA probe against the non-coding sequence of ST-920PC, counterstained with Gill's hematoxylin, shown at 2×–40× magnification (left and right panels show formulation buffer control and high-dose-treated mouse, respectively). Positive hybridization signals are detected as red punctate dots when visualized under bright-field microscopy. (D–G) α-Gal A activities were determined in the (D) plasma and (E) tissues of the treated Fabry mice, as were the percent (%) of (F) Gb3 and (G) Lyso-Gb3 remaining in the plasma and tissues relative to the untreated age- and sex-matched Fabry controls. For (A) and (B), symbols represent individual mice, whereas for (D)–(G), data shown are means + SDs (n = 9, 10, 9, and 20 for the control, 2.0E+12, 5.0E+12, and 5.0E+13 vg/kg groups, respectively). *p < 0.05, **p < 0.01, ***p < 0.001 versus untreated Fabry group, two-way repeated-measures ANOVA followed by Dunnett's multiple comparison test. gDNA = genomic DNA.

ST-920PC/Sf9, an AAV2/6-hGLA Vector Produced by Clinical-Scale Manufacturing, Normalizes Substrates in Key Tissues with No Safety Findings in Fabry Mice

Efforts were then directed to assess the pharmacodynamic activity, efficacy, and safety of ST-920PC/Sf9, an AAV2/6-hGLA vector generated by a clinical-scale manufacturing process using the Sf9/rBV system. A single i.v. administration of ST-920PC/Sf9 into the Fabry mice at a dose of 2.0E+12 (low dose, n = 10), 5.0E+12 (mid dose, n = 10), or 5.0E+13 vg/kg (high dose; n = 20) resulted in dose-dependent increases of mean vector DNA copy number (Figure 4A) and *GLA* mRNA levels (Figure 4B) in liver when assessed 90 days post-treatment.

In line with these findings, a semiquantitative DNA *in situ* hybridization-based assay[29,30] using a probe that specifically detects a non-coding region of the ST-920PC vector showed a positive correlation between vector dose and the percentage of hybridization signal-positive liver cells (Figure 4C, representative data are shown). At 90 days post-injection, the low-dose group mouse (n = 1) had 1.1% positive cells, while the mid- (n = 2) and high-dose (n = 3) group had, on average, 5.0% and 39.3% positive cells, respectively. In contrast, an untreated control animal (n = 1) had background levels of 0.16% positive cells. Vector dose also correlated positively with mean number of positive hybridization signals per liver cell (data not shown).

Dose-related increases in plasma α-Gal A activities were observed 1 week post-injection, and similar levels were sustained through the 3-month duration of the study in all dose groups (Figure 4D). At 85 days post-treatment, mean plasma α-Gal A activities were 13, 130, and 7,749 nmol/h/mL for the low-, mid-, and high-dose groups, respectively, corresponding to a ~1-, 7-, and 408-fold increase relative to mean levels in wild-type mice. Hepatic α-Gal A activities correlated

positively with vector dose, with mean activities of 47, 114, and 13,020 nmol/h/mg for the low-, mid-, and high-dose groups, respectively, corresponding to 5-, 12-, and 1,400-fold increases over mean wild-type activity (Figure 4E). These levels were markedly increased compared with the mean hepatic activity in the formulation buffer-treated Fabry mouse controls, 2.5 nmol/h/mg. Although the low- and mid-dose groups had cardiac and renal α-Gal A activities comparable with untreated controls, Fabry mice administered the high dose had mean cardiac and renal α-Gal A activities of 187 ± 161 and 142 ± 52 nmol/h/mg, corresponding to ~31- and 5-fold increases relative to mean wild-type mouse levels, respectively (Figure 4E). Anti-human α-Gal A antibody titers were determined in plasma by an ELISA-based assay at days 8, 28, 43, and 71 post-injection. There were no significant increases in anti-human α-Gal A antibody levels in any of the treated groups between days 8 and 71, and average antibody levels in treated groups at day 71 were not significantly higher than in the formulation control group (data not shown).

Fabry mice treated with the high dose of ST-920PC/Sf9 had undetectable levels (i.e., below the lower limit of quantitation [LLOQ] for the mass spectrometry assay) of Lyso-Gb3 in plasma and all tissues analyzed, including liver, heart, and kidney, and <10% of Gb3 remaining in plasma and all tissues compared with the Fabry mouse controls (Figures 4F and 4G). Treatment with low and mid ST-920PC/Sf9 doses cleared the majority of Gb3 from the heart (~30% and ~20% Gb3 remaining, respectively); however, these vector doses had less impact on cardiac Lyso-Gb3 levels (~65% and 55% lyso-Gb3 remaining in low- and mid-dose groups, respectively). These doses did not effectively clear substrate in kidney, which retained 80% and 70% of Gb3 and 60% and 51% of Lyso-Gb3 in the low- and mid-dose groups, respectively, compared with Fabry mouse controls. Liver, heart, and kidney tissue samples from wild-type mice had levels of Gb3 and Lyso-Gb3 below the LLOQ (data not shown).

Treatment with ST-920PC/Sf9 was well tolerated in Fabry mice. Daily clinical observations showed that there were no apparent changes in appearance or behavioral abnormalities or clinical observations indicative of health issues. Body weight gain was similar for all treatment groups throughout the study. Blood samples were collected and processed for analysis on the final day of the study (day 90). Hematology, clinical chemistry, gross pathology, and organ weights were within the normal range for these mice (data not shown). There were no differences in aspartate aminotransferase (AST) or alanine transaminase (ALT) levels between treated and control group mice. The US Food and Drug Administration (FDA)-recommended standard list of tissues was collected at necropsy, processed to slides, stained with hematoxylin and eosin, and evaluated by a board-certified veterinary pathologist. There were no toxicological findings related to treatment with ST-920PC/Sf9 up to 5.0E+13 vg/kg, the highest dose tested.

In summary, this 3-month hybrid pharmacology and toxicology study demonstrated that liver-targeted delivery of AAV2/6-hGLA vector produced by a clinical-scale manufacturing process effectively normalized Gb3 and Lyso-Gb3 substrates in kidney and heart of adult Fabry mice. Notably, complete substrate clearance was achieved without immunosuppression. No adverse events were observed up to 5.0E+13 vg/kg, the highest dose tested, supporting the safety of this AAV2/6-hGLA vector.

Clinical Lead Vector ST-920 Results in Higher Transgene Expression Compared with ST-920PC, Both *In Vitro* and *In Vivo*, with No Safety Findings in Wild t-ype C57BL/6 Mice

In an effort to further enhance the potency of the therapeutic AAV2/6-hGLA vector, we generated a vector designated ST-920 in HEK cells (ST-920/HEK), and its pharmacodynamic activity was compared with ST-920PC/HEK in various hepatic primary cells and cell lines. The ST-920 expression cassette is identical in design to ST-920PC, except that it contains an additional 3′ WPRE enhancer element to promote transgene mRNA stability and nuclear export[31,32] (Figure 1). Transduction of human and murine hepatoma cell lines, HepG2 (Figure 5A) and Hepa1-6 (Figure 5B), respectively, non-human primate (NHP, cynomolgus monkey) primary hepatocytes (Figure 5C), iCell human induced pluripotent stem cell (iPSC)-derived hepatocytes (Figure 5D), and two different lots of human primary hepatocytes (Figures 5E and 5F) with ST-920/HEK or ST-920PC/HEK resulted in dose-dependent increases of α-Gal A activity in the cell culture supernatants at 3–9 days post-transduction. ST-920/HEK resulted in supernatant α-Gal A activities that were generally 2- to 10-fold higher than ST-920PC/HEK in all cell lines tested, with the greatest differences observed at the highest vector doses (i.e., 1E+5 to 1.2E+6 vg/cell).

The ST-920 vector was then produced using a clinical manufacturing process utilizing the Sf9/rBV expression system (ST-920/Sf9), and *in vivo* pharmacodynamic activity was directly compared with ST-920PC/Sf9, the vector evaluated in the Fabry mouse hybrid 3-month pharmacology and toxicology study, in wild-type C57/BL6 male mice. Three vector doses were tested, 5.0E+12 and 5.0E+13 vg/kg, the mid and high doses used in the Fabry mouse hybrid pharmacology and toxicology study, respectively, and 1.5E+14 vg/kg, which was tested only for the ST-920 vector. At 29 days following vector administration, dose-related increases in vector copy numbers were detected in liver of both ST-920/Sf9- and ST-920PC/Sf9-treated groups. The ST-920/Sf9 and ST-920PC/Sf9 groups administered 5.0E+12 and 5.0E+13 vg/kg had comparable vector copies per dose in liver (Figure 6A), indicating that transduction efficiency of the two vectors was similar.

Dose-dependent increases in plasma α-Gal A activity were detected by day 8 post-injection and were sustained for the 1-month duration of the study (Figure 6B). At day 29 post-injection, mean plasma α-Gal A activity levels in the ST-920/Sf9-treated mice were 470, 30,269, and 83,659 nmol/h/mL, in order of ascending vector dose, corresponding to 24-, 1,568-, and 4,335-fold increases relative to the untreated C57BL/6 control group, respectively (mean day 29 plasma activity in untreated control group = 19.3 nmol/h/mL; Figure 6B). These levels were up to 7-fold higher than those achieved with ST-920PC/Sf9, which were 301 and 4297 nmol/h/mL at the

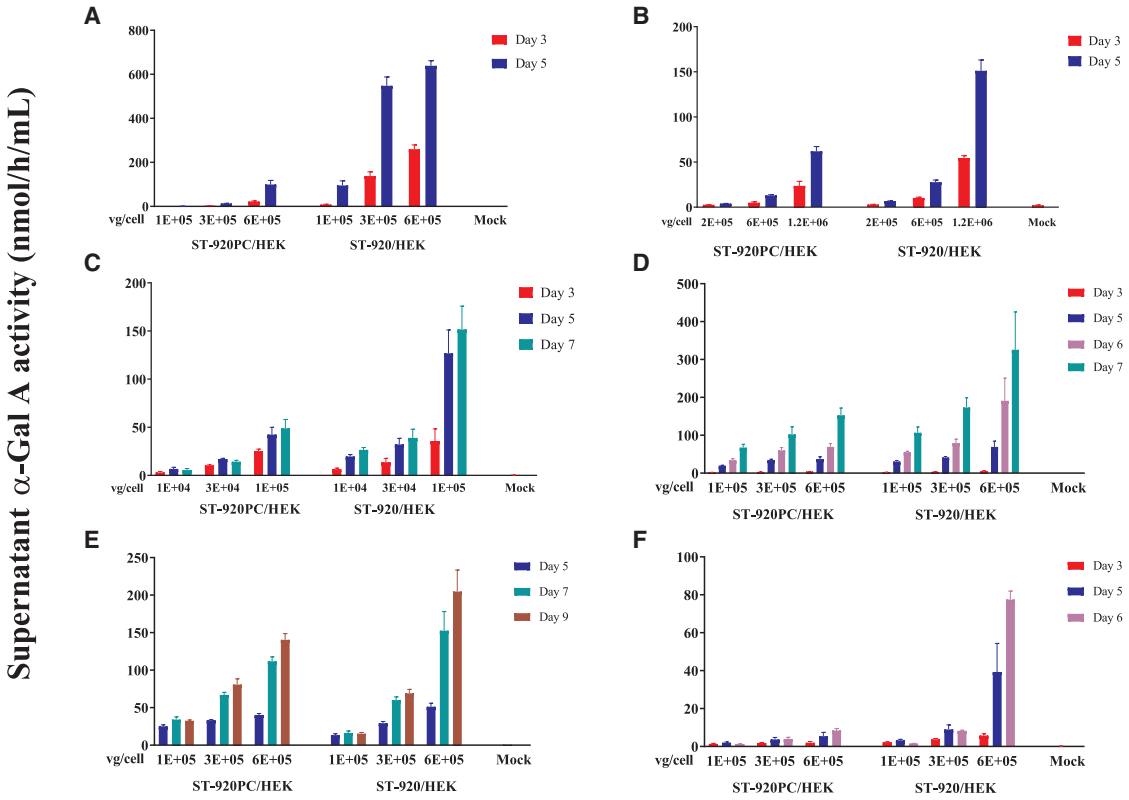

Figure 5. ST-920/HEK Produces Higher Levels of Actively Secreted α-Gal A Enzyme Compared with ST-920PC/HEK *In Vitro*

(A–F) α-Gal A activities in supernatants of ST-920PC/HEK- or ST-920/HEK-transduced (A) HepG2 and (B) Hepa1-6, which are human and mouse hepatoma cell lines, respectively, (C) non-human primate (NHP) primary hepatocytes, (D) iCells human iPSC-derived hepatocytes, and two different lots of human primary hepatocytes: (E) lot HUM180871, and (F) lot 380. Cells were transduced with indicated vector doses (vg/cell), and supernatants were collected and assayed for α-Gal A activities on days 3, 5, 6, 7, and/or 9 post-transduction. Mock-transduced wells were administered formulation buffer without AAV vector. Data presented are means ± SD of three biological replicates.

5.0E+12 and 5.0E+13 vg/kg doses, respectively. α-Gal A activity determined in liver homogenates at day 29 post-injection showed a similar profile, with ST-920/Sf9 having ~2-fold and 7-fold higher activity than ST-920PC/Sf9 at the 5.0E+12 and 5.0E+13 vg/kg doses, respectively (Figure 6C). Thus, both *in vitro* and *in vivo* studies showed increased pharmacodynamic activity of ST-920 compared with ST-920PC.

To evaluate the potential toxicity of ST-920/Sf9, we conducted a separate 1-month Good Laboratory Practice (GLP) toxicology study in C57BL/6 wild-type male mice using the same ST-920/Sf9 vector lot as used in the pharmacology study described above. Following i.v. administration of ST-920/Sf9 at doses of 5.0E+12, 5.0E+13, and 1.5E+14 vg/kg (n = 10/group), mice were assessed for daily clinical observations, weekly body weights, hematology and serum chemistry parameters (samples collected on day 29), and gross pathology at necropsy. The FDA-recommended standard set of tissues was collected, processed to slides, stained with hematoxylin and eosin, and evaluated by a board-certified veterinary pathologist. Liver samples were also collected for exposure assessment/biodistribution at necropsy.

At 29 days post-treatment, mean vector copy numbers in liver and mean plasma α-Gal A activity were comparable with those in the study above (Figures S2A and S2B), thus confirming that liver was efficiently transduced.

Administration of ST-920/Sf9 was well tolerated, with the no-observed-adverse-effect-level (NOAEL) being the highest dose tested, 1.5E+14 vg/kg. All experimental mice survived to scheduled euthanasia, and there were no apparent clinical signs of toxicity. There were no test article-related changes in hematology, clinical chemistry, and macroscopic and microscopic pathology. There were no treatment-related abnormalities following i.v. administration of ST-920/Sf9 at dose levels up to 1.5E+14 vg/kg, the highest dose tested.

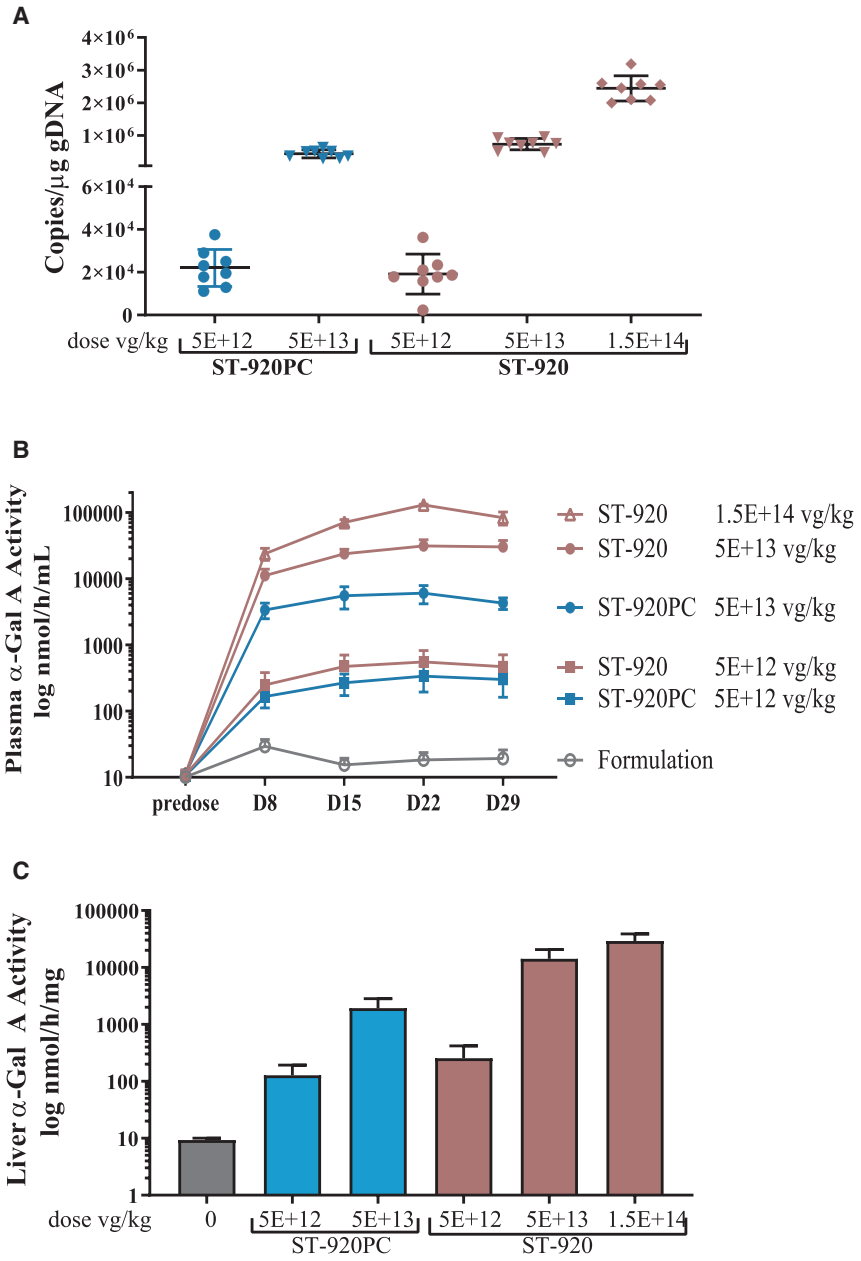

Figure 6. ST-920/Sf9 Is More Efficacious Than ST-920PC/Sf9 *In Vivo*

ST-920/Sf9 or ST-920PC/Sf9 was i.v. administered to wild-type C57BL/6 males at doses of 5E+12, 5E+13, or 1.5E+14 vg/kg, and tissues were collected at day 29 post-injection. Liver vg copy numbers of the individual mice (A) and α-Gal A activities in plasma (B) and the liver (C), shown as means ± SEMs, are presented (n = 4 for formulation buffer controls, n = 8 for all other groups). gDNA = genomic DNA.

Taken together, these data show that treatment with the ST-920 vector was safe and more potent than ST-920PC. Of note, the ST-920PC vector essentially normalized Gb3 and Lyso-Gb3 concentrations in adult Fabry mice in heart and kidney, the key sites of pathology in patients with Fabry disease. Thus, these studies support ST-920 as the lead clinical candidate to be evaluated in a phase I/II clinical study for treatment of Fabry disease.

DISCUSSION

Clinical application of AAV-based vectors for liver-targeted *in vivo* gene therapy has rapidly increased over the last decade, largely because of the good safety profile of these vectors and the success of recent clinical trials for hemophilia A and B using AAV-mediated approaches.[33–35] Although a number of clinical trials are currently ongoing to evaluate the efficacy and safety of liver-targeted AAV gene therapy for various inherited metabolic diseases, including ornithine transcarbamylase (OTC) deficiency, Crigler-Najjar syndrome, Pompe disease, mucopolysaccharidosis (MPS) type IIIA, glycogen storage disease type Ia, and aromatic L-amino acid decarboxylase deficiency, prior to 2019 there were no clinical studies to assess this therapeutic approach for Fabry disease. Previous preclinical evaluation of AAV2- and AAV1-mediated gene therapy approaches in the Fabry mice (*Gla* KO) showed sub-optimal substrate clearance in key target tissues, particularly the kidney.[28,36,37] The use of an AAV8 vector markedly improved transgene expression, but normalization of renal Gb3 was achieved only when the Fabry mice were treated at a young age (1 month old), before the onset of significant disease pathology.[27] Therefore, we sought to design a highly effective AAV2/6-hGLA vector to establish proof of concept for clinical development of a liver-targeted gene therapy approach for Fabry disease.

We demonstrated in adult Fabry mice (2–3 months old) that liver-directed AAV2/6-hGLA gene therapy produced by a clinical-scale manufacturing process, ST-920PC/Sf9, markedly increased α-Gal A expression in liver (up to 1,400-fold over wild-type levels; Figure 4E), resulting in its abundant secretion into the circulation (up to 408-fold over wild type; Figure 4D). The secreted α-Gal A enzyme was effectively taken up by the target tissues, such as the kidney and heart, leading to clearance of glycolipid substrates, Gb3 and Lyso-Gb3, when treated with 5.0E+13 vg/kg ST-920PC/Sf9 (Figures 4F and 4G). *In vitro* studies indicated that tissue uptake of liver-expressed α-Gal A enzyme is mediated by M6P receptors, because uptake of enzyme in various cell lines was inhibited in

the presence of excess M6P (Figure 3F). In contrast, at the low and mid doses (2.0E+12 and 5.0E+12 vg/kg, respectively), only partial substrate clearance was achieved in these tissues despite hepatic α-Gal A activities being increased to levels that were ~5 and ~12-fold over wild-type levels, whereas plasma activities were elevated ~1 and ~7-fold over wild-type levels (Figures 4D and 4E). These findings are consistent with previous studies demonstrating that markedly high intracellular overexpression of normal α-Gal A is necessary to induce the selective secretion of the M6P-conjugated enzyme.[38] Importantly, detailed hematology, clinical chemistry, macroscopic, and histological assessment over a 3-month period support the safety of ST-920PC/Sf9 *in vivo*.

It was notable that the ST-920PC/Sf9 vector resulted in lower plasma α-Gal A activities compared with hGLApoc/VV (Figures 2B and 4D), which was used for the initial 6-month proof-of-concept study, at equivalent vector doses. Presumably, this was due to differences in the Sf9/rBV systems (i.e., small-scale versus clinical-scale production) used to generate the two vector lots, because the ST-920PC expression cassette was more potent than hGLApoc, both *in vitro* and *in vivo*, when compared head-to-head using the same vector manufacturing protocol (Figures 3A and 3B).

Subsequent efforts were directed to improve the transgene expression cassette design to further enhance AAV2/6-hGLA-mediated α-Gal A expression in plasma and tissues. The *GLA* cDNA sequence used in ST-920PC was optimized; thus, efforts focused on evaluating the impact of adding an enhancer element to the 3′ end of the transgene expression cassette. Both *in vitro* and *in vivo* studies demonstrated that addition of a 3′ WPRE to the expression cassette (new construct designated ST-920) significantly increased (up to 7-fold) α-Gal A activity in plasma (Figure 6B) and liver (Figure 6C) compared with ST-920PC, whereas transduction efficiency was unchanged (Figure 6A). Maximizing the potency of the therapeutic AAV vector is of critical importance for clinical applications, because previous studies have shown that transducing liver cells in larger animals, such as NHP, is significantly more challenging compared with mice, with a 50- to 100-fold decreased transduction efficiency.[39,40] Additionally, a more potent vector would permit use of a lower vector dose, potentially allowing the vector to circumvent or minimize anti-AAV capsid immune responses, which are associated with administration of higher vector doses.[40] Of note, previous studies in transgenic mice overexpressing α-Gal A have demonstrated the safety of excess systemic α-Gal A activity levels, up to 155- and 44-fold in the plasma and liver, respectively.[41]

ST-920/Sf9 was well tolerated and showed no adverse effects in a 1-month GLP toxicology study in wild-type C57BL/6 male mice, at dose levels up 1.5E+14 vg/kg, the highest dose tested. For reference, this dose is 5-fold higher than the highest administered dose (3E+13 vg/kg) of SB-525, an AAV6 vector for treating hemophilia A, which is currently undergoing evaluation in a phase I/II clinical trial and to date has a good safety profile. ST-920/Sf9 was rapidly cleared from the bloodstream and other biological fluids, including the urine and saliva (data not shown).

A safe and effective AAV2/6-hGLA-mediated gene therapy approach offers several advantages over ERT, the current standard treatment for Fabry disease. Most importantly, gene therapy has the potential to be a one-time treatment, whereas ERT necessitates lifelong 2- to 4-h biweekly infusions. Additionally, a number of studies demonstrate the potential of AAV gene therapy to induce immune tolerance against the therapeutic target protein, while with ERT, the formation of neutralizing antibodies against the recombinant enzyme remains an issue.[18,19,42] We showed that AAV2/6-hGLA-treated Fabry mice sustained markedly increased α-Gal A activity in plasma without immunosuppression, suggesting that they do not generate significant levels of neutralizing antibodies against the liver-produced human enzyme (Figure 4D). Consistent with this finding, anti-α-Gal A antibody titers measured by an ELISA-based assay were not significantly increased in treated groups compared with the control group in the plasma of Fabry mice in the 3-month pharmacology and toxicology study (data not shown). Further, AAV-mediated gene therapy in mouse models of hemophilia B and Pompe disease with pre-existing antibodies to the respective therapeutic proteins led to persistent reduction or elimination of the antibodies.[25,43,44] If true in humans, this would be a significant advantage, because it would permit the treatment of Fabry patients with pre-existing α-Gal A antibodies (resulting from ERT) with AAV gene therapy.

In summary, the feasibility of expressing durable and therapeutic levels of α-Gal A using clinical-scale manufactured AAV2/6-hGLA vectors was demonstrated in preclinical studies. The highly optimized final lead vector, ST-920, resulted in the highest plasma and tissue transgene expression and demonstrated a good safety profile in Fabry and wild-type mice. Together, these studies provide the foundation for a phase I/II clinical trial to evaluate the safety and efficacy of ST-920, a liver-targeted AAV2/6-mediated gene therapy approach, in patients with Fabry disease.

MATERIALS AND METHODS

AAV2/6 Vector Production

All AAV2/6-hGLA vectors had a transgene expression cassette containing a liver-specific promoter and enhancer, a chimeric intron, and a codon-optimized full-length h*GLA* cDNA, including the native *GLA* signal peptide (amino acids 1–31). AAV2/6-hGLA vectors were produced using one of the following three manufacturing systems: (1) a nonclinical, small-scale Sf9/rBV expression system using methods proprietary to contracted research organization (CRO) Virovek (vectors designated [vector name]/VV); (2) a Sf9/rBV-based clinical manufacturing process[45] (designated [vector name/Sf9]); or (3) a triple-transfection system in HEK cells (designated [vector name]/HEK). Triple transfection of HEK cells was performed in 10-layer CellSTACK chambers (Corning, Corning, NY, USA). AAV2/6-hGLA vectors were diluted into formulation buffer, consisting of phosphate-buffered saline (PBS) supplemented with 35 mM NaCl, 1% sucrose, and 0.05% Pluronic F-68. AAV titers were determined by quantitative polymerase chain reaction (qPCR).[46]

In Vitro Transduction of Hepatic Cell Lines and Primary Hepatocytes

HepG2/C3A (CRL-10741; ATCC, Manassas, VA, USA) and Hepa1-6 cells (CRL-1830; ATCC) were maintained in Minimum Essential Medium (MEM; Corning) with 10% fetal bovine serum (FBS; Life Technologies, Carlsbad, CA, USA) and 1× penicillin-streptomycin-glutamine (Life Technologies) and incubated at 37°C with 5% CO_2. Cells were passaged every 3–4 days.

Human primary hepatocytes (Lot No. HUM180871; Lonza, Basel, Switzerland and Corning human hepatocytes Lot No. 380), cynomolgus monkey primary hepatocytes (male cynomolgus monkey platable hepatocytes, Lot No. BBD; BioIVT, Westbury, NY, USA), and iCell human iPSC-derived hepatocytes (Lot No. 1029; Fujifilm Cellular Dynamics, Madison, WI, USA) were thawed and recovered in the vendor-established medium (Table S1). Cells were transferred from the liquid nitrogen vapor phase directly into a 37°C water bath and thawed under gentle stirring. Cell viability was determined using trypan blue solution, and the cells were plated and maintained in the specified growth medium (Table S1) at 37°C with 5% CO_2. At 70%–80% confluency, cells were rinsed and trypsinized with 0.25% Trypsin/2.21 mM ethylenediaminetetraacetic acid (EDTA) (Corning) and re-suspended in growth or maintenance media. A small aliquot was mixed 1:1 with trypan blue solution 0.4% (w/v) in PBS (Corning), and cells were counted on the TC20 Automated Cell Counter (Bio-Rad, Hercules, CA, USA). The cells were re-suspended and seeded into a 24- or 48-well plate (Corning) at the indicated cell density (Table S1) in 0.5 or 0.3 mL media per well, respectively.

Transductions were performed 1 day after cell plating. AAV2/6-hGLA particles were mixed at the appropriate multiplicity of infection (MOI) with growth or maintenance media and added to the cells. Cells were transduced in biological replicates of three at MOI doses ranging from 1E+4 to 1.2E+6 vg/cell, as specified. Media were exchanged at day 3 post-transduction. Cell culture supernatants were collected at the indicated time points post-transduction and frozen at −80°C until use.

Cellular Uptake of AAV2/6-hGLA-Expressed α-Gal A Enzyme

K562 human leukemia cells (ATCC; CCL-243) were maintained in MEM with 10% FBS (Life Technologies) and 1× penicillin-streptomycin-glutamine (Life Technologies). Fabry mouse-derived immortalized aortic endothelial cells (FMEC2) were maintained in culture flasks coated with 0.1% gelatin (Millipore, Burlington, MA, USA) in media consisting of Dulbecco's modified Eagle's medium (DMEM; Corning) with 20% FBS (Life Technologies), 25 mM HEPES (Thermo Fisher Scientific, Waltham, MA, USA), 1× nonessential amino acids (Sigma-Aldrich, St. Louis, MO, USA), 100 μg/mL heparin (Sigma-Aldrich), 50 μg/mL endothelial cell growth supplement (Sigma-Aldrich), and 1× penicillin-streptomycin-glutamine (Life Technologies). Fabry patient fibroblasts were cultured in DMEM with 10% FBS. Cells were incubated at 37°C with 5% CO_2 and passaged every 3–7 days.

HepG2 cells were transduced with ST-920PC/HEK at an MOI of 6.0E+5 vg/cell. Supernatant was collected 5 days post-transduction, and its markedly elevated α-Gal A activity was confirmed. K562 and FMEC2 cells and Fabry patient fibroblasts were cultured for 24 h in the presence of the α-Gal A enriched HepG2 cell supernatant, with or without 5 mM mannose 6-phosphate (M6P). Cell pellets were collected and assessed for α-Gal A activity using the procedures described. Supernatant from mock-transduced HepG2 cells served as a negative control.

Preclinical Studies in the Fabry Mice and Wild-Type C57BL/6 Mice

Fabry mice (*Gla* KO) were maintained in a barrier facility at the Icahn School of Medicine at Mount Sinai. All animal procedures were reviewed and approved by the Icahn School of Medicine at Mount Sinai's Internal Animal Care and Use Committee (IACUC). AAV2/6-hGLA vectors were diluted in formulation buffer so that each mouse received 10 μL/g body weight, and then were injected into the tail veins of 8- to 12-week-old male mice (day 1). For the initial 6-month proof-of-concept study, the Fabry mice were immunosuppressed once every 2 weeks with intraperitoneal injections of cyclophosphamide (50 mg/kg) starting the day before vector administration (day 0). Subsequent studies did not use immune suppression. Blood samples were collected in EDTA K2-coated tubes from facial veins, and plasma was isolated by centrifugation at 2,500 × *g* for 10 min. Mice were sacrificed at the indicated times by perfusion with PBS via the left ventricle under ketamine/xylazine anesthesia, and tissues were snap frozen in liquid nitrogen and stored at −80°C until use. Tissue samples were homogenized in Promega chilled reporter lysis buffer (Madison, WI, USA), and protein concentrations were determined using the Bio-Rad Bradford Protein Assay. The 1-month studies using wild-type C57BL/6 males (8–10 weeks old) were performed at the CRO, Pacific Biolabs (Hercules, CA, USA).

genomic DNA Purification and Vector Genome Quantitation

genomic DNA was isolated from liver and testes (~15 mg tissue per sample) using the QIAGEN DNeasy Blood and Tissue Kit (Hilden, Germany), according to the manufacturer's instructions. DNA concentrations were determined using a dye-binding method.[47] AAV2/6-hGLA vg copy numbers were determined by TaqMan qPCR using an oligonucleotide primer pair that amplified a fragment in the AAV2/6-hGLA vector backbone and a probe dually labeled with the 6-carboxyfluorescein (FAM) reporter dye on its 5′ end and the non-fluorescent Black Hole Quencher-1 on its 3′ end (forward primer 5′-GCAAACATTGCAAGCAGCAA-3′, reverse primer 5′-TGCCCC AGCTCCAAGGT-3′, and probe 5′-CAAACACACAGCCCTCCC TGCCTG-3′). PCR amplification was performed using the following cycling conditions: 2 min at 50°C, 10 min at 95°C, followed by 40 cycles of 30 s at 95°C and 1 min at 60°C, and FAM signals were detected on a QuantStudio 3 real-time PCR system (Thermo Fisher Scientific). To generate the standard curve, eight-point serial dilutions of the AAV2/6-hGLA reference standard were each mixed with 300 ng mouse genomic DNA, and qPCR was performed as described above. Data were processed using QuantStudio Design and Analysis

software and expressed as vg copies per micrograms genomic DNA. Lower limits of quantitation were 150 and 100 vg copies/μg genomic DNA for the liver and testes, respectively.

Quantification of *GLA* mRNA in Livers

Total RNA was purified from homogenized liver tissue using the QIAGEN AllPrep DNA/RNA Mini Kit, and cDNA was synthesized using the QIAGEN QuantiTect Reverse Transcription kit, according to the manufacturer's protocol. qPCR was performed using the SsoFast master mix (Bio-Rad) and a custom primer/probe mix targeting the ST-920PC *GLA* cDNA transgene (forward primer 5′- CGTT GAAAGACCTGCTGTAATC-3′, reverse primer 5′-CAGATGGCT GGCAACTAGAA-3′, and probe 5′-CTGCAGGAATTCGGCTCGA GATCC-3′). Serially diluted linearized ST-920PC plasmid DNA (1.0E+6, 2.5E+5, 6.25E+4, 15,625, 3,906.25, 976.56, 244.14, or 61.04 copies) was used to generate a standard curve. mRNAs from four AAV2/6-hGLA-treated mice (one from each dose group) were directly added to PCRs, without first performing the RT step, as negative controls.

α-Gal A Enzymatic Activity Assays

α-Gal A activities were assessed using a previously described fluorescence-based enzymatic activity assay[48] with the following modifications. Working stocks for 4-methylumbelliferyl (4MU) and recombinant human α-Gal A enzyme, which served as a positive control, were prepared by spiking 4MU or α-Gal A enzyme into 100% heat-inactivated pooled male mouse plasma to concentrations of 3,645 nmol/h/mL and 4,000 ng/mL, respectively. On the day of the experiment, standard and product curves were generated by initially diluting the working stocks to a minimal required dilution of 1:10 in assay diluent, followed by serial dilution into 10% of the same pooled plasma.

Cell culture medium or cell lysate, or mouse plasma or tissue lysate, was diluted at 1:10 (liver) or 1:5 (other tissues) in assay diluent, and 10 μL of the diluted sample was added into a well of a 96-well nonbinding plate. Per well, 40 μL of a substrate/inhibitor master mix consisting of 1M 4MU-alpha-D-galactopyranoside (4MU-α-Gal; Sigma-Aldrich, St. Louis, MO, USA), dissolved in assay buffer (0.2 M citrate, 0.4 M phosphate buffer [pH 4.4]), and 2.5 mM *N*-acetylgalactosamine[49] (Sigma-Aldrich), an α-galactosidase B inhibitor, was added, and the plate was incubated for 60 min at 37°C with shaking (~100 rpm). The plate was then removed from the shaker, and 100 μL of 0.5 M glycine [pH 10.2] was added per well to stop the reaction. For each well, 100 μL of the total reaction volume was transferred from the clear reaction plate to a flat-bottom black plate, and the amount of 4MU produced was analyzed on the SpectraMax i3X reader (365 nm excitation, 450 nm emission) using SoftMax Pro 7.0. α-Gal A activities were calculated based on the 4MU standard curve and expressed as nanomoles of 4MU released per hour per milliliter (nmol/h/mL) for plasma and culture media samples, and nanomoles of 4MU released per hour per milligram protein (nmol/h/mg protein) for tissue and cell lysates. The assay's LLOQ was 2.5 nmol/h/mL (plasma) and 2 nmol/h/mg (tissues).

Plasma and Tissue Gb3 and Lyso-Gb3 Quantitation

Tissue and plasma Gb3 and Lyso-Gb3 concentrations were determined using liquid chromatography-mass spectrometry (LC-MS) at Brains-Online (Charles River Laboratories, Wilmington, MA, USA) or inVentiv Health Clinical Lab (Syneos Health, Raleigh, NC, USA). For assays performed at Brains-Online, the following methodology was used: in brief, tissues (1 mg) were homogenized in 9 μL methanol (MeOH) containing 0.1% formic acid using a glass bead homogenizer. Plasma (1 μL) was mixed with 9 μL of 100% MeOH. Tissue or plasma samples were mixed for 30 min on an orbital shaker and then centrifuged at 13,000 rpm for 30 min. The supernatants, containing Gb3 and Lyso-Gb3, were diluted in MeOH and mixed with internal standards containing glucosyl (β) sphingosine (GSG) and Gb3 (C23:0). 5 μL of the processed tissue or plasma sample was injected into an integrated liquid chromatography-tandem mass spectrometry (LC-MS/MS) system, containing prominence series LC system (Shimadzu, Kyoto, Japan) and an API4000 triple-quadrupole MS system (AB Sciex, Foster City, CA, USA). The mixture was separated on a Kinetex C18 column 50 × 2.1 mm, 1.7 μm (Phenomenex, Torrance, CA, USA), using a linear gradient starting with 40% of MeOH in water and ending with 100% MeOH. The analytes were detected in positive ionization mode, with the following transitions: for Lyso-Gb3, 786.8 → 282.4; and for Gb3 (C24:0), 1,137.8 → 264.4. An external calibration curve was run in matched matrix containing Lyso-Gb3 (Avanti Polar, Alabaster, AL, USA) and Gb3 (Matreya, State College, PA, USA). Quantitation was done using Analyst 1.4.2 (AB Sciex).

For assays performed at inVentiv, the following methodology was used: in brief, the samples are extracted using a liquid-liquid extraction procedure followed by LC/ESI/MS/MS (Liquid Chromatography Electrospray Ionization Tandem Mass Spectrometric) detection in positive ion mode. Quantitation was based on the detection and integration of the product ion traces using Analyst 1.6 (Applied Biosystems/MDS Sciex). All regressions and calculations on the area integrations were performed through a validated in-house-developed macro spreadsheet, Samp Calc (version 4), in Microsoft Excel using system default values.

Western Blot Analysis in Cell Culture Supernatants and Liver Homogenates

Frozen liver tissue (~50 mg) was homogenized in 500 μL radioimmunoprecipitation (RIPA) buffer supplemented with HALT Protease Inhibitor (Thermo Fisher Scientific), using Lysis Matrix D tubes and a FastPrep 24 Instrument (both from MP Biomedicals, Burlingame, CA, USA) for five rounds (pulse time 45 s, velocity 4.5 m/s). Crude liver lysates were centrifuged at 14,000 rpm for 10 min at 4°C, and protein concentrations were determined in the clarified lysates using the Pierce bicinchoninic acid (BCA) Protein Assay Kit (Thermo Fisher Scientific).

Aliquots of liver lysates or HepG2 supernatants were digested with EndoH (New England Biolabs, Ipswich, MA, USA) or PNGase F (New England Biolabs) using the manufacturer's protocol. EndoH cleaves within the chitobiose core of high mannose and some hybrid oligosaccharides from N-linked glycoproteins such as α-Gal A.

PNGase F cleaves the innermost *N*-acetylglucosamine and asparagine residues of high mannose, hybrid, and complex oligosaccharides, thus removing nearly all N-linked oligosaccharides from the protein.

Under denaturing conditions, 10 μL HepG2 supernatant or total protein (35 μg) from liver homogenates was separated on 4%–12% NuPAGE Novex Bis Tris gels (Life Technologies) and immobilized on a nitrocellulose membrane. The membranes were blocked with Odyssey Blocking Buffer (LI-COR Biotechnology, Lincoln, NE, USA) for 1 h at room temperature, then incubated overnight at 4°C with polyclonal goat anti-(α-Gal A) antibodies (R&D Systems, Minneapolis, MN, USA), diluted 1:1,000 in Odyssey Blocking Buffer. Following five washes, membranes were probed with polyclonal donkey anti-[goat IgG (H+L)] antibodies conjugated with IRDye 680RD (LI-COR Biotechnology), diluted 1:10,000 in Odyssey Blocking Buffer, for 1 h at room temperature. Membranes were washed five times for 5 min in Tris-buffered saline, 0.1% Tween 20 (TBST) and then probed with an anti-heat shock protein 90 (anti-HSP90) antibody conjugated to DyLight 800, using the Lightning Link conjugation kit (Novus Biologicals, Littleton, CO, USA), for 1 h at room temperature. Images were captured using a LI-COR Odyssey scanner.

Semiquantitative DNA *In Situ* Hybridization-Based Assay to Evaluate Transduction Efficiency

Transduction efficiency of the ST-920PC/Sf9 vector was evaluated in Fabry mouse livers using the BaseScope Red v.2 Reagent Kit (Advanced Cell Diagnostics, Newark, CA, USA) and an oligonucleotide probe that specifically detects a non-coding region of the ST-920PC vector, according to the manufacturer's protocol. In brief, liver tissues were mounted on slides and pretreated for antigen retrieval, and then hybridized with the ST-920PC-targeted probe. Following a series of washes to amplify the signal, we performed signal detection via a chromogenic substrate, which produces a precipitate that is visible as a distinct red dot under common brightfield microscopy at 10–20× magnification. Quantitative analysis was conducted using HALO software. Slides were counterstained with Gill's hematoxylin using standard procedures.

Statistical Analysis

Statistical analyses were performed using two-way repeated-measures ANOVA followed by Dunnett's multiple comparison test and conducted on GraphPad Prism software version 8.4.

SUPPLEMENTAL INFORMATION

Supplemental Information can be found online at https://doi.org/10.1016/j.omtm.2020.07.002.

AUTHOR CONTRIBUTIONS

Conceptualization, M.W.H., M.C.H., and T.W.; Methodology, M.Y., M.W.H., S.P., R.J.D., and T.W.; Investigation, M.Y., M.W.H., S.P., L.G., S.S.M., S.S., D.R., S.B., K.H., and A.L.; Writing, M.Y., M.W.H., and R.J.D.; Supervision, M.Y., L.F., L.C., Y.L., M.C.H., K.M., R.J.D., and T.W.

CONFLICTS OF INTEREST

M.W.H., S.S.M., D.R., S.B., K.H., A.L., L.F., L.C., Y.L., M.C.H., K.M., and T.W. are full-time employees and/or shareholders of Sangamo Therapeutics. M.Y., S.P., and R.J.D. received funding from Sangamo Therapeutics to perform some of the animal studies.

ACKNOWLEDGMENTS

The authors are grateful to Carolyn Gasper, Eudean Garces, Andres Villegas, Marina Falaleeva, and Judy Greengard for their contributions to designing and overseeing the conduct of the animal studies and sample analysis. The authors would also like to thank Dr. Raphael Schiffmann and Dr. Jinsong Shen for kindly providing the Fabry mouse endothelial cells and Fabry patient fibroblast cells used in the α-Gal A uptake experiments.

REFERENCES

1. Desnick, R.J., Ioanou, Y.A., and Eng, C.M. (2001). α-Galactosidase A deficiency: Fabry disease. In The Metabolic and Molecular Bases of Inherited Disease, C.R. Scriver, A.L. Beaudet, W.S. Sly, D. Valle, K.E. Kinzler, and B. Volgelstein, eds. (McGraw-Hill), pp. 3733–3774.
2. Aerts, J.M., Groener, J.E., Kuiper, S., Donker-Koopman, W.E., Strijland, A., Ottenhoff, R., van Roomen, C., Mirzaian, M., Wijburg, F.A., Linthorst, G.E., et al. (2008). Elevated globotriaosylsphingosine is a hallmark of Fabry disease. Proc. Natl. Acad. Sci. USA *105*, 2812–2817.
3. Elleder, M. (2008). Cellular and tissue localization of globotriaosylceramide in Fabry disease. Virchows Arch. *452*, 705–author reply 707–708.
4. Thurberg, B.L., Fallon, J.T., Mitchell, R., Aretz, T., Gordon, R.E., and O'Callaghan, M.W. (2009). Cardiac microvascular pathology in Fabry disease: evaluation of endomyocardial biopsies before and after enzyme replacement therapy. Circulation *119*, 2561–2567.
5. Thurberg, B.L., Rennke, H., Colvin, R.B., Dikman, S., Gordon, R.E., Collins, A.B., Desnick, R.J., and O'Callaghan, M. (2002). Globotriaosylceramide accumulation in the Fabry kidney is cleared from multiple cell types after enzyme replacement therapy. Kidney Int. *62*, 1933–1946.
6. Desnick, R.J., and Banikazemi, M. (2006). Fabry disease: clinical spectrum and evidence-based enzyme replacement therapy. Nephrol. Ther. *2* (*Suppl 2*), S172–S185.
7. Desnick, R.J., and Wasserstein, M.P. (2001). Fabry disease: clinical features and recent advances in enzyme replacement therapy. Adv. Nephrol. Necker Hosp. *31*, 317–339.
8. Nakao, S., Kodama, C., Takenaka, T., Tanaka, A., Yasumoto, Y., Yoshida, A., Kanzaki, T., Enriquez, A.L., Eng, C.M., Tanaka, H., et al. (2003). Fabry disease: detection of undiagnosed hemodialysis patients and identification of a "renal variant" phenotype. Kidney Int. *64*, 801–807.
9. von Scheidt, W., Eng, C.M., Fitzmaurice, T.F., Erdmann, E., Hübner, G., Olsen, E.G., Christomanou, H., Kandolf, R., Bishop, D.F., and Desnick, R.J. (1991). An atypical variant of Fabry's disease with manifestations confined to the myocardium. N. Engl. J. Med. *324*, 395–399.
10. Nakao, S., Takenaka, T., Maeda, M., Kodama, C., Tanaka, A., Tahara, M., Yoshida, A., Kuriyama, M., Hayashibe, H., Sakuraba, H., et al. (1995). An atypical variant of Fabry's disease in men with left ventricular hypertrophy. N. Engl. J. Med. *333*, 288–293.
11. Echevarria, L., Benistan, K., Toussaint, A., Dubourg, O., Hagege, A.A., Eladari, D., Jabbour, F., Beldjord, C., De Mazancourt, P., and Germain, D.P. (2016). X-chromosome inactivation in female patients with Fabry disease. Clin. Genet. *89*, 44–54.
12. Eng, C.M., Banikazemi, M., Gordon, R.E., Goldman, M., Phelps, R., Kim, L., Gass, A., Winston, J., Dikman, S., Fallon, J.T., et al. (2001). A phase 1/2 clinical trial of enzyme replacement in fabry disease: pharmacokinetic, substrate clearance, and safety studies. Am. J. Hum. Genet. *68*, 711–722.
13. Eng, C.M., Guffon, N., Wilcox, W.R., Germain, D.P., Lee, P., Waldek, S., Caplan, L., Linthorst, G.E., and Desnick, R.J.; International Collaborative Fabry Disease Study

Group (2001). Safety and efficacy of recombinant human alpha-galactosidase A replacement therapy in Fabry's disease. N. Engl. J. Med. *345*, 9–16.

14. Germain, D.P., Charrow, J., Desnick, R.J., Guffon, N., Kempf, J., Lachmann, R.H., Lemay, R., Linthorst, G.E., Packman, S., Scott, C.R., et al. (2015). Ten-year outcome of enzyme replacement therapy with agalsidase beta in patients with Fabry disease. J. Med. Genet. *52*, 353–358.

15. Desnick, R.J., Brady, R., Barranger, J., Collins, A.J., Germain, D.P., Goldman, M., Grabowski, G., Packman, S., and Wilcox, W.R. (2003). Fabry disease, an under-recognized multisystemic disorder: expert recommendations for diagnosis, management, and enzyme replacement therapy. Ann. Intern. Med. *138*, 338–346.

16. Germain, D.P., Elliott, P.M., Falissard, B., Fomin, V.V., Hilz, M.J., Jovanovic, A., Kantola, I., Linhart, A., Mignani, R., Namdar, M., et al. (2019). The effect of enzyme replacement therapy on clinical outcomes in male patients with Fabry disease: A systematic literature review by a European panel of experts. Mol. Genet. Metab. Rep. *19*, 100454.

17. Ortiz, A., Germain, D.P., Desnick, R.J., Politei, J., Mauer, M., Burlina, A., Eng, C., Hopkin, R.J., Laney, D., Linhart, A., et al. (2018). Fabry disease revisited: Management and treatment recommendations for adult patients. Mol. Genet. Metab. *123*, 416–427.

18. Lenders, M., Stypmann, J., Duning, T., Schmitz, B., Brand, S.M., and Brand, E. (2016). Serum-Mediated Inhibition of Enzyme Replacement Therapy in Fabry Disease. J. Am. Soc. Nephrol. *27*, 256–264.

19. Linthorst, G.E., Hollak, C.E., Donker-Koopman, W.E., Strijland, A., and Aerts, J.M. (2004). Enzyme therapy for Fabry disease: neutralizing antibodies toward agalsidase alpha and beta. Kidney Int. *66*, 1589–1595.

20. Germain, D.P., Hughes, D.A., Nicholls, K., Bichet, D.G., Giugliani, R., Wilcox, W.R., Feliciani, C., Shankar, S.P., Ezgu, F., Amartino, H., et al. (2016). Treatment of Fabry's Disease with the Pharmacologic Chaperone Migalastat. N. Engl. J. Med. *375*, 545–555.

21. Benjamin, E.R., Della Valle, M.C., Wu, X., Katz, E., Pruthi, F., Bond, S., Bronfin, B., Williams, H., Yu, J., Bichet, D.G., et al. (2017). The validation of pharmacogenetics for the identification of Fabry patients to be treated with migalastat. Genet. Med. *19*, 430–438.

22. Lukas, J., Giese, A.K., Markoff, A., Grittner, U., Kolodny, E., Mascher, H., Lackner, K.J., Meyer, W., Wree, P., Saviouk, V., and Rolfs, A. (2013). Functional characterisation of alpha-galactosidase a mutations as a basis for a new classification system in fabry disease. PLoS Genet. *9*, e1003632.

23. Wu, X., Katz, E., Della Valle, M.C., Mascioli, K., Flanagan, J.J., Castelli, J.P., Schiffmann, R., Boudes, P., Lockhart, D.J., Valenzano, K.J., and Benjamin, E.R. (2011). A pharmacogenetic approach to identify mutant forms of α-galactosidase A that respond to a pharmacological chaperone for Fabry disease. Hum. Mutat. *32*, 965–977.

24. Lheriteau, E., Davidoff, A.M., and Nathwani, A.C. (2015). Haemophilia gene therapy: Progress and challenges. Blood Rev. *29*, 321–328.

25. Ioannou, Y.A., Zeidner, K.M., Gordon, R.E., and Desnick, R.J. (2001). Fabry disease: preclinical studies demonstrate the effectiveness of alpha-galactosidase A replacement in enzyme-deficient mice. Am. J. Hum. Genet. *68*, 14–25.

26. Lemansky, P., Bishop, D.F., Desnick, R.J., Hasilik, A., and von Figura, K. (1987). Synthesis and processing of alpha-galactosidase A in human fibroblasts. Evidence for different mutations in Fabry disease. J. Biol. Chem. *262*, 2062–2065.

27. Ziegler, R.J., Cherry, M., Barbon, C.M., Li, C., Bercury, S.D., Armentano, D., Desnick, R.J., and Cheng, S.H. (2007). Correction of the Biochemical and Functional Deficits in Fabry Mice Following AAV8-mediated Hepatic Expression of alpha-galactosidase A. Mol. Ther. *15*, 492–500.

28. Ziegler, R.J., Lonning, S.M., Armentano, D., Li, C., Souza, D.W., Cherry, M., Ford, C., Barbon, C.M., Desnick, R.J., Gao, G., et al. (2004). AAV2 vector harboring a liver-restricted promoter facilitates sustained expression of therapeutic levels of alpha-galactosidase A and the induction of immune tolerance in Fabry mice. Mol. Ther. *9*, 231–240.

29. Wang, F., Flanagan, J., Su, N., Wang, L.C., Bui, S., Nielson, A., Wu, X., Vo, H.T., Ma, X.J., and Luo, Y. (2012). RNAscope: a novel in situ RNA analysis platform for formalin-fixed, paraffin-embedded tissues. J. Mol. Diagn. *14*, 22–29.

30. Wang, Z., Portier, B.P., Gruver, A.M., Bui, S., Wang, H., Su, N., Vo, H.T., Ma, X.J., Luo, Y., Budd, G.T., and Tubbs, R.R. (2013). Automated quantitative RNA in situ hybridization for resolution of equivocal and heterogeneous ERBB2 (HER2) status in invasive breast carcinoma. J. Mol. Diagn. *15*, 210–219.

31. Donello, J.E., Loeb, J.E., and Hope, T.J. (1998). Woodchuck hepatitis virus contains a tripartite posttranscriptional regulatory element. J. Virol. *72*, 5085–5092.

32. Zanta-Boussif, M.A., Charrier, S., Brice-Ouzet, A., Martin, S., Opolon, P., Thrasher, A.J., Hope, T.J., and Galy, A. (2009). Validation of a mutated PRE sequence allowing high and sustained transgene expression while abrogating WHV-X protein synthesis: application to the gene therapy of WAS. Gene Ther. *16*, 605–619.

33. Nathwani, A.C., Reiss, U.M., Tuddenham, E.G., Rosales, C., Chowdary, P., McIntosh, J., Della Peruta, M., Lheriteau, E., Patel, N., Raj, D., et al. (2014). Long-term safety and efficacy of factor IX gene therapy in hemophilia B. N. Engl. J. Med. *371*, 1994–2004.

34. Nathwani, A.C., Tuddenham, E.G., Rangarajan, S., Rosales, C., McIntosh, J., Linch, D.C., Chowdary, P., Riddell, A., Pie, A.J., Harrington, C., et al. (2011). Adenovirus-associated virus vector-mediated gene transfer in hemophilia B. N. Engl. J. Med. *365*, 2357–2365.

35. Rangarajan, S., Walsh, L., Lester, W., Perry, D., Madan, B., Laffan, M., Yu, H., Vettermann, C., Pierce, G.F., Wong, W.Y., and Pasi, K.J. (2017). AAV5-Factor VIII Gene Transfer in Severe Hemophilia A. N. Engl. J. Med. *377*, 2519–2530.

36. Jung, S.C., Han, I.P., Limaye, A., Xu, R., Gelderman, M.P., Zerfas, P., Tirumalai, K., Murray, G.J., During, M.J., Brady, R.O., and Qasba, P. (2001). Adeno-associated viral vector-mediated gene transfer results in long-term enzymatic and functional correction in multiple organs of Fabry mice. Proc. Natl. Acad. Sci. USA *98*, 2676–2681.

37. Ogawa, K., Hirai, Y., Ishizaki, M., Takahashi, H., Hanawa, H., Fukunaga, Y., and Shimada, T. (2009). Long-term inhibition of glycosphingolipid accumulation in Fabry model mice by a single systemic injection of AAV1 vector in the neonatal period. Mol. Genet. Metab. *96*, 91–96.

38. Ioannou, Y.A., Bishop, D.F., and Desnick, R.J. (1992). Overexpression of human alpha-galactosidase A results in its intracellular aggregation, crystallization in lysosomes, and selective secretion. J. Cell Biol. *119*, 1137–1150.

39. Nietupski, J.B., Hurlbut, G.D., Ziegler, R.J., Chu, Q., Hodges, B.L., Ashe, K.M., Bree, M., Cheng, S.H., Gregory, R.J., Marshall, J., and Scheule, R.K. (2011). Systemic administration of AAV8-α-galactosidase A induces humoral tolerance in nonhuman primates despite low hepatic expression. Mol. Ther. *19*, 1999–2011.

40. Colella, P., Ronzitti, G., and Mingozzi, F. (2017). Emerging Issues in AAV-Mediated *In Vivo* Gene Therapy. Mol. Ther. Methods Clin. Dev. *8*, 87–104.

41. Ashley, G.A., Desnick, R.J., Gordon, R.E., and Gordon, J.W. (2002). High overexpression of the human alpha-galactosidase A gene driven by its promoter in transgenic mice: implications for the treatment of Fabry disease. J. Investig. Med. *50*, 185–192.

42. van der Veen, S.J., van Kuilenburg, A.B.P., Hollak, C.E.M., Kaijen, P.H.P., Voorberg, J., and Langeveld, M. (2019). Antibodies against recombinant alpha-galactosidase A in Fabry disease: Subclass analysis and impact on response to treatment. Mol. Genet. Metab. *126*, 162–168.

43. Kishnani, P.S., and Koeberl, D.D. (2019). Liver depot gene therapy for Pompe disease. Ann. Transl. Med. *7*, 288.

44. Harding, T.C., Koprivnikar, K.E., Tu, G.H., Zayek, N., Lew, S., Subramanian, A., Sivakumaran, A., Frey, D., Ho, K., VanRoey, M.J., et al. (2004). Intravenous administration of an AAV-2 vector for the expression of factor IX in mice and a dog model of hemophilia B. Gene Ther. *11*, 204–213.

45. Urabe, M., Ding, C., and Kotin, R.M. (2002). Insect cells as a factory to produce adeno-associated virus type 2 vectors. Hum. Gene Ther. *13*, 1935–1943.

46. Sharma, R., Anguela, X.M., Doyon, Y., Wechsler, T., DeKelver, R.C., Sproul, S., Paschon, D.E., Miller, J.C., Davidson, R.J., Shivak, D., et al. (2015). In vivo genome editing of the albumin locus as a platform for protein replacement therapy. Blood *126*, 1777–1784.

47. Simbolo, M., Gottardi, M., Corbo, V., Fassan, M., Mafficini, A., Malpeli, G., Lawlor, R.T., and Scarpa, A. (2013). DNA qualification workflow for next generation sequencing of histopathological samples. PLoS ONE *8*, e62692.

48. Desnick, R.J., Allen, K.Y., Desnick, S.J., Raman, M.K., Bernlohr, R.W., and Krivit, W. (1973). Fabry's disease: enzymatic diagnosis of hemizygotes and heterozygotes. Alpha-galactosidase activities in plasma, serum, urine, and leukocytes. J. Lab. Clin. Med. *81*, 157–171.

49. Mayes, J.S., Scheerer, J.B., Sifers, R.N., and Donaldson, M.L. (1981). Differential assay for lysosomal alpha-galactosidases in human tissues and its application to Fabry's disease. Clin. Chim. Acta *112*, 247–251.